The Eastasouth Journal of Information System and Computer Science
Vol. 3, No. 03, April 2026, pp. 397-409
ISSN: 3025-566X, DOI: 10.58812/esiscs.v3i03

Autonomous Thermo-Mechanical Co-Design of Embedded Liquid-Cooling Structures for High-Power Mobility Platforms: A Systematic Review

Rupesh Rameshrao Dhore
Senior Design Release Engineer, Solize USA Corporation, Canton, MI, USA

Article Info

Article history:

Received April, 2026
Revised April, 2026
Accepted April, 2026

Keywords:

Adjoint Sensitivity;
Cold Plate;
Conjugate Heat Transfer;
Electric Vehicle Power Electronics;
Liquid Cooling;
Pin-Fin Heat Sink;
Thermo-Mechanical Co-Design;
Topology Optimization

ABSTRACT

For electric traction inverters and onboard electronics that adopt wide-bandgap switches, bus bars and capacitors to increasingly shrink packages, embedded liquid-cooling structures are a key enabler for power density. Based on 20 peer-reviewed papers published from 2005 to 2025, this systematic review aims to explore the merging of autonomous, optimization-based design approaches with thermo-mechanical requirements for these structures. The corpus was coded on the basis of considering the following aspects: physics fidelity, design representation, optimization algorithm, validation route and application context. Combined with adjoint sensitivity analysis, pseudo-three-dimensional reduced-order models and extensions to the adjoint model for transient and turbulent flow, the density-based topology optimization with Brinkman penalization will emerge as the predominant autonomous design engine. Results indicate that the optimised fin array reduced pressure loss by almost 53.6% compared with circular fins, the pseudo-three dimensional heat sink lowered the thermal resistance by up to 13.6% compared with optimised size parallel fin, the transient design reduced the pumping power by 66.7% and the hybrid topology-microchannel cold plate reduced the peak chip temperature by 4.28K with a pressure drop of 319.42Pa. Traditional cooling technology uses 14% to 33% of the traction-inverter volume, making it evident that the value of compact, co-designed structures is high. There are still some structural compliance, thermal-cycling fatigue, manufacturability in optimization loops and limitation in treatment. A co-design framework with closed loop coupling is proposed to guide future development: mission profiles, reduced order solvers, adjoint updates and experimental verification.

This is an open access article under the CC BY-SA license.

Corresponding Author:

Name: Rupesh Rameshrao Dhore
Institution: Senior Design Release Engineer, Solize USA Corporation, Canton, MI, USA
Email: rupeshdhorey@gmail.com

1. INTRODUCTION

Current high power mobility systems, such as Battery Electric Vehicles, Hybrid drivetrains and automated vehicles with high density onboard computing, requires thermal loads conventional air-cooled hardware can't handle. Embedded liquid-cooling structures which consist of coolant passages, fins and pins mounted directly in a baseplate or housing are therefore considered as part of the power-conversion

system and not as accessories. Thermo-mechanical co-design refers to the design of coolant-path topology at the same time as solid architecture, in which thermal, hydraulic and structural requirements are all satisfied in the same design loop. Micro pin-fin studies with circular, hydrofoil, modified hydrofoil and symmetric convex-lens pins are used to illustrate the severity of the challenge, as peak temperature and peak pressure penalty were important and dominated by pin shape in the tests for background fluxes of the order of 500 W/cm2 and localized hot spots close to 2000 W/cm2 [1].

To the extent that the term is used in this review, autonomous design involves computational methods that produce geometries for cooling from a given design space, given boundary conditions and objectives, with minimal human intervention. In problems involving fluid, such autonomy is the main tool exploited, namely topology optimization (TO) is a process that distributes material in a domain to extremize a performance measure. A thorough review resulted in the identification of 186 papers published between 2003 and January 2020, and the compilation of these papers into five families: pure fluid flow, species transport, conjugate heat transfer, fluid-structure interaction, and microstructure and porous media. From that same survey, it was noted that most of the contributions dealt with the steady laminar flow and that the problems of transient and turbulent flow need to be given more attention [2].

Geometric design is the one variable that designers have the greatest control over. A focused study of micro heat sinks has demonstrated that the parameters: cross section of the channel, shape and pitch of the pins, flow interruption, and channel inlet and outlet arrangement influence the balance between heat transfer enhancement and hydraulic loss differently, and that the parameters interact nonlinearly with one another, meaning that sequential manual tuning rarely finds a global compromise [3]. With this background, the present review has three aims: First, to summarise the mathematical formulations that have been used to support autonomous cooling design; Second, to compare optimization strategies and their validated performance; and Third, to outline the steps required to advance the discussion of thermo-fluid optimization to true thermo-mechanical co-design for mobility applications. This review method, the governing formulations, optimization strategies, application context, adjoint and transient autonomy, experimental evidence and critical discussion is presented in the following sections.

2. REVIEW METHODOLOGY

A set of 20 peer-reviewed sources (publications) were selected and subjected to a structured review protocol from 2005-2025. These sources were resolved across five attributes: physics fidelity, design representation, optimization algorithm, validation route and application context. The sources were then categorised by method type into 5 method families: reviews/surveys, parametric design, evolutionary design, steady density based TO, transient, turbulent and adjoint formulations, and cold plate experiments and simulations. The first source was to combine design of experiments sampling method with central composite and response surface designs, and adding gradient search to the optimization of confined pin-fin heat sinks with consideration of pressure drop, mass and space constraints [4]. The baseline is used as a benchmark to measure future design freedoms. The resultant literature map is summarised in Table 1, and the distribution of the corpus over the five families is illustrated in Figure 1.

Table 1. Literature Map of the Reviewed Corpus

Ref.	Year	Focus	Method	Key reported outcome
[1]	2015	Micro pin-fin arrays with a hot spot	3D conjugate CFD of four pin shapes	Pin shape governs peak temperature and pressure drop under 500/2000 W/cm² loading

Ref.	Year	Focus	Method	Key reported outcome
[2]	2020	Fluid-based TO	Survey of 186 papers (2003–2020)	Steady laminar flow dominates; transient and turbulent work flagged as priorities
[3]	2020	Micro heat sink geometry	Review	Channel shape, pin layout and manifolds govern the thermo-hydraulic trade-off
[4]	2005	Pin-fin heat sink design	DOE, CCD and RSM with gradient search	Constrained optima under pressure-drop, mass and space limits
[5]	2017	TO of heat transfer systems	Review	Density approach most widely adopted for convective design
[6]	2011	Unsteady Navier–Stokes TO	Density-based, transient adjoint	Time-dependent objectives handled consistently
[7]	2018	Turbulent heat sink TO	Density-based, k–ω RANS, automatic differentiation	Turbulent forced convection made tractable
[8]	2020	Fin-array power loss	Pseudo-spectral Brinkman TO, Re 2–50	Up to 53.6% lower pressure loss than circular fins
[9]	2021	Pin-fin heat exchangers	Multi-objective TO, spectral and finite-element	Topology outperforms pure sizing optimization
[10]	2018	Forced-convection heat sink	Pseudo-3D density-based TO	Up to 13.6% lower thermal resistance
[11]	2012	Pin-fin geometry	Multi-objective GA, Bézier profile	Pareto set of fin profiles
[12]	2022	EV traction power electronics	Review	Cooling occupies 14%–33% of inverter volume
[13]	2008	Plate-fin versus pin-fin	Experiments and correlations	Preferred type depends on pumping power and length
[14]	2013	Viscous flow with heat transfer	Continuous adjoint, constrained TO	Gradient cost independent of design-variable count
[15]	2011	Unsteady flow	Density-based TO	Transient objectives and sensitivities
[16]	2019	Liquid-cooled heat sink	TO, CNC prototypes, experiments	Flow-distribution and heat-exchange designs versus S-channel
[17]	2019	Liquid-cooled heat sink	Multi-objective TO, 3D CHT, experiments	Lower thermal resistance and higher Nu than parallel channel
[18]	2024	High-voltage EV inverter	Parametric pin-fin CFD	Pin number, size and flow rate assessed
[19]	2025	Chip cold plate	TO integrated with microchannels	−4.28 K peak temperature; −319.42 Pa pressure drop
[20]	2020	Instantaneous chip cooling	Transient pseudo-3D TO	66.7% lower pumping power

Note: TO = topology optimization; DOE = design of experiments; CCD = central composite design; RSM = response surface method; CHT = conjugate heat transfer.

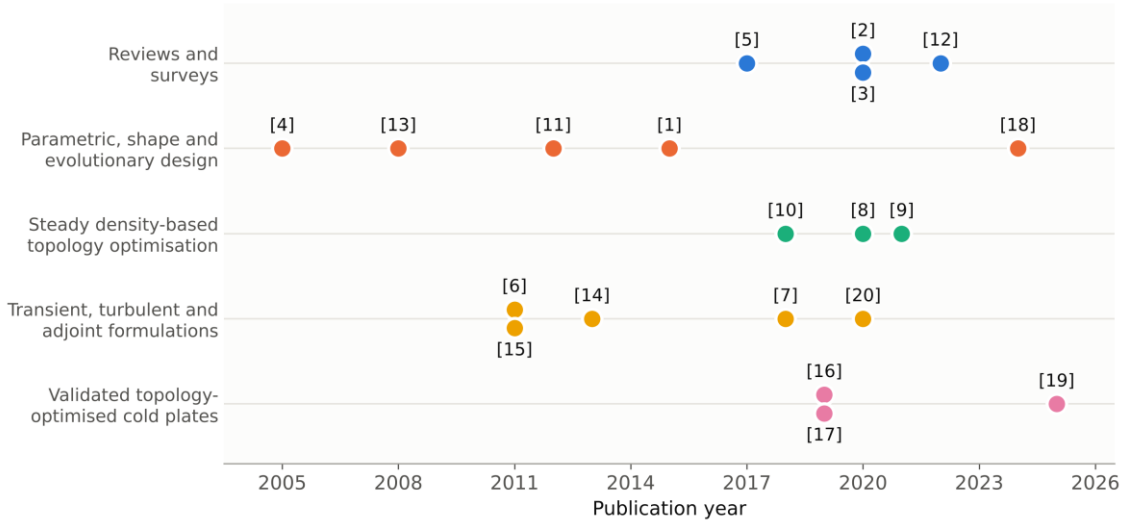


Figure 1. Temporal Distribution of the Reviewed Corpus Across Five Methodological Families
Note: markers show reference numbers; stacked markers denote two studies in the same year.

3. GOVERNING FORMULATIONS FOR THERMOFLUID CO-DESIGN

3.1 *Density-Based Design Representation*

The density approach is the most common representation used for convective problems discussed in the literature for optimal design of a heat transfer system, since it can be applied to design the fluid-solid layout without the need to track boundaries on a fixed mesh [5]. Each element is given a continuous design variable $\gamma \in [0, 1]$ where $\gamma = 0$ corresponds to solid and $\gamma = 1$ corresponds to fluid. The Brinkman friction term $\alpha(\gamma)$ is used to suppress flow in solid areas, and is approximated by a rational approximation of material properties (RAMP) with convexity parameter q. The resulting steady incompressible problem is given in (1) to (4) where u is velocity, p is pressure, ϱ is density, μ is dynamic viscosity, cp is specific heat, k(γ) is the interpolated thermal conductivity, T is temperature and Q is the volumetric heat source.

$$\nabla \cdot u = 0 \quad (1)$$

$$\rho(u \cdot \nabla)u = -\nabla p + \mu\nabla^2 u - \alpha(\gamma)u \quad (2)$$

$$\alpha(\gamma) = \alpha_{\max} + (\alpha_{\min} - \alpha_{\max})\frac{\gamma(1+q)}{\gamma+q} \quad (3)$$

$$\rho c_p u \cdot \nabla T = \nabla \cdot (k(\gamma)\nabla T) + Q \quad (4)$$

3.2 *Transient and Turbulent Extensions*

Steady formulations ignore the load transients of mobility duty cycles, which include sudden bursts of acceleration, and regenerative braking. The extension to the optimization of a density of unsteady incompressible Navier-Stokes flow showed that time-dependent objective functions can be dealt with by numerically summing the cost over the simulation time and by numerically solving an adjoint system backward in time [6]. A representative transient objective for a cooling structure subjected to a pulsed loss profile is the time averaged mean temperature of the heated base region Ωb for the time interval 0 - tf, as defined in (5) above. This is a significant computational cost, as the forward solution needs to be saved or solved again for the backward sweep.

$$\Phi_T = \frac{1}{t_f|\Omega_b|}\int_0^{t_f}\int_{\Omega_b} T \, d\Omega \, dt \quad (5)$$

Coolant flow in vehicles is often done at Reynolds numbers at which the laminar assumptions are not necessarily valid. The Reynolds-averaged Navier–Stokes equations were solved along with a turbulent k–ω turbulence model while penalising turbulence quantities in the solid domain, and the exact sensitivities were obtained using automatic

differentiation [7] to optimise the density of heat sinks under turbulent forced convection. This advances a major fidelity hurdle in auto cold plates, but makes each iteration of the design much more costly. Table 2 compares the main formulations and their physics, cost and suitability, while Figure 2 shows how the parameter q in (3) dictates the sharpness of the transition between the solid-like and fluid-like behaviours, and hence the level of convergence and the existence of intermediate densities.

Table 2. Comparison of Thermofluid Formulations Used for Autonomous Cooling Design

Formulation	Physics captured	Relative cost	Main limitation	Mobility use	Refs.
Steady 2D density-based	Laminar flow with convection-diffusion	Low	No out-of-plane conduction	Concept screening	[2], [5]
Pseudo-3D two-layer	Design layer coupled to conducting base	Low to moderate	Fixed channel height; calibrated coupling	Cold-plate layout	[9], [10], [20]
Unsteady / transient	Time-dependent flow and heat	High	Storage for backward adjoint sweep	Drive-cycle pulses	[6], [15], [20]
Turbulent RANS (k–ω)	Turbulence-affected transport	High	Wall treatment in density setting	High-flow coolant loops	[7]
Constrained continuous adjoint	Viscous flow and heat with constraints	Moderate per gradient	Derivation effort	Multi-constraint design	[14]
Full 3D body-fitted	Complete conjugate physics	Very high	Rarely used inside the loop	Final verification	[10], [17]

Note: relative cost is a qualitative ranking synthesized from the reported model descriptions.

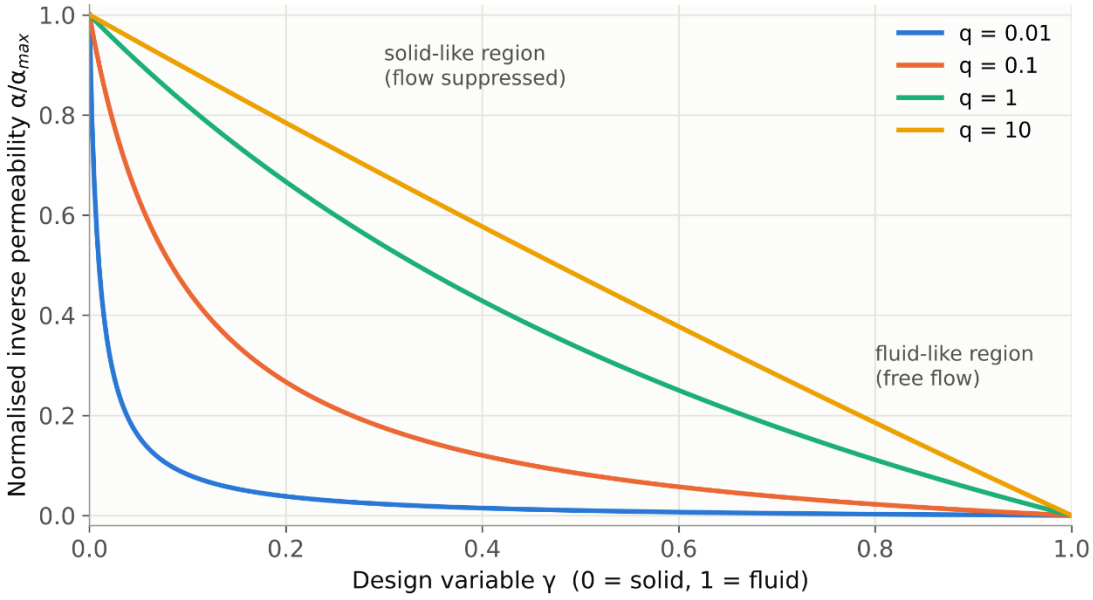


Figure 2. Effect of the RAMP Convexity Parameter on the Brinkman Inverse-Permeability Interpolation

Note: curves computed from the RAMP interpolation in (3) with α_min = 0.

4. OPTIMIZATION STRATEGIES AND DESIGN FREEDOM

4.1 *Gradient-Based Topology Optimization*

The first cost of any embedded cooling structure is the loss of pressure; pumping power is being taken from the same vehicle energy store that it protects. An approach of minimising the power loss of the flow across the fin array was developed using a density-based method and a pseudo-spectral solver with Brinkman penalization for flow around doubly periodic two-dimensional domains, for Reynolds number ranging from 2 to 50 [8]. Optimized staggered arrays also resulted in a 12.61% decrease in pressure loss at Re = 2 and 53.58% at Re = 50 when compared to the circular fins, whereas in-line and staggered arrays at Re = 25 resulted in a decrease of about 39% and 39.45% respectively. Optimized aspect ratios were seen to have increased from 1.99 to 3.63 as compared to circular fins. The memory usage was up to 18 GB and the time needed for each iteration on a 128 × 128 grid was 15 to 20 min. The comparison of the two cases is shown in Figure 3, and the objective of dissipated power is given in (6).

$$\Phi_f = \int_\Omega \left[\frac{\mu}{2}\|\nabla u + \nabla u^{\mathrm{T}}\|^2 + \alpha(\gamma)\|u\|^2\right] \mathrm{d}\Omega \quad (6)$$

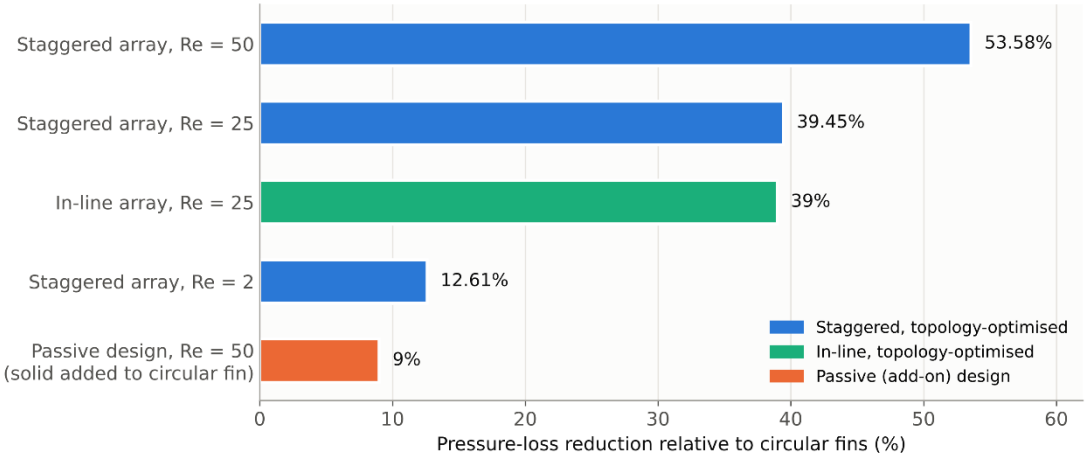


Figure 3. Pressure-Loss Reductions of Topology-Optimized Fin Arrays Relative to Circular Fins

Note: values reported for two-dimensional periodic arrays.

In the case of dense pin fin sinks, thermal resistance and pressure loss are conflicting requirements, making it impossible to achieve a solution with just one of these objectives. A multi-objective formulation for pin-fin heat exchangers was developed using a pseudo-spectral periodic flow solver, a finite-element conjugate heat transfer model, and was shown to attain a significant reduction in thermal resistance while minimizing pressure loss simultaneously from both in-line and staggered configurations, and compared to pure sizing optimization, TO was demonstrated to outperform the latter in both cases [9]. The metrics are considered to be: the thermal resistance (7), the pumping power (8) and the normalized weighted-sum objective (9) with constraints (10), where Tmax is the maximum base temperature, Tin is the coolant inlet temperature, Q̇ is the dissipated heat, V̇ is the pumping volumetric flow rate, wt and wf are the thermal weight and hydraulic weight, and V∗ is the admissible fluid volume fraction. The Pareto front is swept from zero to one in wt.

$$R_{\mathrm{th}} = \frac{T_{\max} - T_{\mathrm{in}}}{\dot{Q}} \quad (7)$$

$$P_{\mathrm{pump}} = \Delta p\, \dot{V} \quad (8)$$

$$\min_{\gamma} \Phi = w_t \frac{\Phi_T}{\Phi_{T,0}} + w_f \frac{\Phi_f}{\Phi_{f,0}} \quad (9)$$

$$\frac{1}{|\Omega|}\int_\Omega \gamma \,\mathrm{d}\Omega \le V^*,\ w_t + w_f = 1 \quad (10)$$

4.2 Reduced-Order and Evolutionary Alternatives

The pseudo-three-dimensional model came about because full three-dimensional optimization is still too costly for routine design. The two dimensional thermofluidic design layer in this model is thermally coupled with the two dimensional conducting base plate, periodic thermofluidic designs are obtained due to symmetry conditions and the goal is to minimize heat transfer resistance for a given pressure drop and heat generation [10]. Validation with body-fitted 2-D and 3-D simulations was done and a good match was obtained, and two designs with thermal resistance optimization resulted in a maximum reduction of 13.6% compared to a size-optimized parallel-fin design. An effective convection coefficient heff in (11) represents the interlayer coupling, where Tb and Td are the base-layer and design-layer temperatures, respectively, and qc is the exchanged heat flux.

$$q_c = h_{\text{eff}}(T_b - T_d) \quad (11)$$

Where objectives are discontinuous, or design spaces are small, gradient-free alternatives are still applicable. A multi-objective genetic algorithm (GA) was used to optimize the geometry of the pin-fins, where the geometry of the pin-fin was parameterized by Bézier curves and multiple thermal performance measures were optimized and presented as a Pareto set of profiles [11]. This evolutionary search is powerful, has been easily parallelized, and, as is the case with most evolutionary searches, the cost is dependent on the number of design variables making them impractical for the number of element-wise densities that can be used by the gradient-based TO. Based on the design freedom, gradient requirement, computational burden and representative outcome, the four strategy families found in the corpus are compared in Table 3.

Table 3. Comparison of Optimization Strategy Families

Strategy	Design variables	Gradient	Computational burden	Representative outcome	Refs.
DOE–RSM with gradient search	Handful of sizing parameters	Surrogate-based	Low	Constrained pin-fin optima	[4]
Multi-objective GA	Profile control points	Not required	Moderate to high (population × solves)	Pareto set of fin profiles	[11]
Density-based TO (MMA)	One density per element	Adjoint	Moderate per iteration	Up to 13.6% lower thermal resistance	[10]
Spectral periodic TO	Grid densities (128 × 128)	Analytical	15–20 min per iteration; up to 18 GB	Up to 53.6% lower pressure loss	[8], [9]

Note: MMA = method of moving asymptotes.

5. APPLICATION CONTEXT: HIGH-POWER MOBILITY PLATFORMS

The most challenging embedded-cooling application on today's vehicles is traction inverters. The most important heat sources are semiconductor switches, but bus bars, power capacitors also generate heat and need to be cooled, and high temperatures speed up failure modes that reduce power-electronic reliability. The dominant architectures are indirect, direct and double-sided, and make up 14-33% of the total volume of inverters, and package size keeps decreasing with increased dissipation [12]. This volume share makes co-designed cooling structures with multiple functions as cooling

structures, mechanical support, and carrier of electrical insulation highly attractive. The main architectures and their implications for autonomous co-design are compared in Table 4.

Table 4. Embedded Cooling Architectures for Traction Power Electronics and Co-Design Opportunities

Architecture	Heat path	Key advantage	Key constraint	Co-design opportunity	Refs.
Indirect	Module, interface material, cold plate	Simple sealing; modular	Interface resistance	Channel topology of the cold plate	[12], [17]
Direct pin-fin baseplate	Module baseplate fins in coolant	No interface layer; large wetted area	Sealing and pressure drop	Pin shape and layout via TO	[8], [9], [18]
Double-sided	Both module faces	Shortest junction-to-coolant path	Mechanical stack complexity	Coupled thermal–structural design	[12]
Plate-fin channels	Parallel channels	Low loss at low pumping power	Lower area density	Regime-based selection	[13]
Hybrid TO plus microchannel	Optimized region feeding straight channels	Uniformity with low pressure drop	Fine-feature manufacture	Integrated layout	[19]

Note: architectures are grouped according to the classification reported for current electric vehicles.

Before detailed optimization, the choice of which of the basic fin families should be selected should be automated. Correlation studies have been conducted on the comparison of optimized plate-fin and pin-fin heat sinks under a fixed pumping power, and the following comparison under the above conditions has been found: When the dimensionless pumping power is small, and length is large, plate-fin heat sink designs have lower thermal resistance, on the other hand, when length is small, and dimensionless pumping power is large, pin-fin heat sink designs have lower thermal resistance [13]. This regime dependence (see the schematic illustration in Figure 4) suggests that the operating point, which is a function of pump power and packaging length, should be found first and then the topology optimization should be seeded with an appropriate initial layout, since the initial guess is known to affect the converged topology.

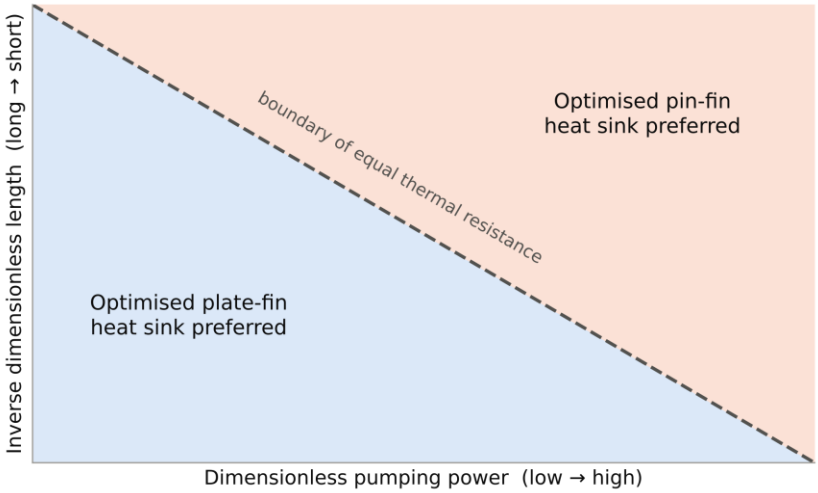


Figure 4. Schematic Regime Map for Selecting Plate-Fin or Pin-Fin Heat Sinks at Fixed Pumping Power

Note: qualitative representation; the boundary position depends on the correlations used.

6. ADJOINT AND TRANSIENT DESIGN AUTONOMY

The autonomous design is scalable if the cost (and number of required sensors) of obtaining sensitivities does not increase with the number of design variables. The continuous adjoint method has been developed for constrained TO of viscous flows with heat transfer, where the objective and the constraint gradients are calculated from a single adjoint solution for each function, in spite of the fact that there are several porosity variables [14]. The total derivative is of the form (12), where R is the discretized state residuals and λ is the adjoint variables. A structural constraint, namely a solid isotropic material with penalization (SIMP) stiffness interpolation with penalty exponent ps, as defined in (13), and a compliance limit C∗, as defined in (14), can be added to the thermal-hydraulic problem, such that thin features are discouraged when the coolant pressure and clamping loads are applied.

$$\frac{\mathrm{d}\Phi}{\mathrm{d}\gamma} = \frac{\partial\Phi}{\partial\gamma} + \lambda^{\mathrm{T}}\frac{\partial R}{\partial\gamma} \quad (12)$$

$$E(\gamma) = E_{\min} + (1-\gamma)^{p_s}(E_0 - E_{\min}) \quad (13)$$

$$C = f^{\mathrm{T}}u_s \leq C^* \quad (14)$$

The flow field also has transient properties, as the operation of the pumps is pulsating, and flow rate changes are also rapid, which affects the effective heat transfer. TO for unsteady flow has been found to produce designs that are different from steady state designs, and that a sensitivity analysis can be carried out consistently within a density framework [15]. Based on these adjoint and transient properties, a closed-loop co-design framework is proposed in Figure 5, which is derived from the reviewed methods. Loss maps and hot-spot layouts are provided by mission profiles, a reduced-order model is used to evaluate the coupled flow, heat and structural response, the adjoint sensitivities are used to obtain filtered and projected updates by the method of moving asymptotes (MMA), and converged Pareto designs are tested by body-fitted three-dimensional analysis and prototype testing prior to feeding back to the mission model via the adjoint sensitivities.

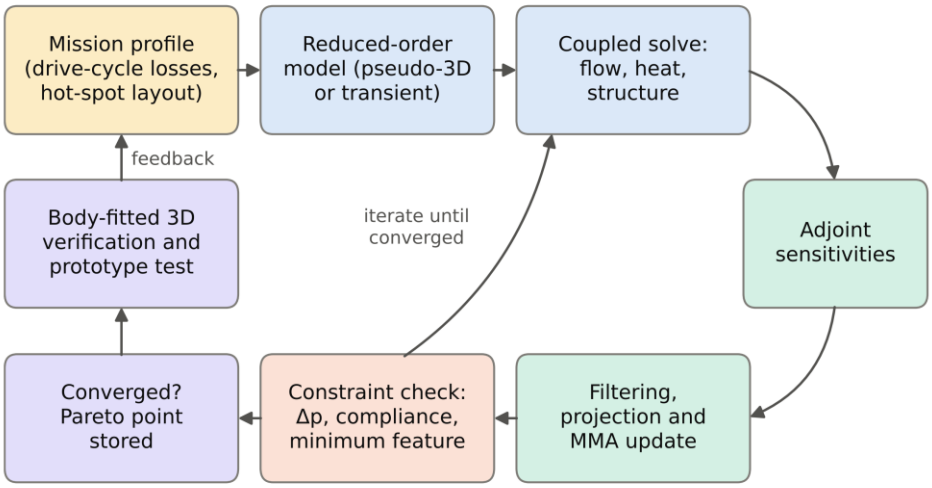


Figure 5. Proposed Closed-Loop Framework for Autonomous Thermo-Mechanical Co-Design
Note: framework synthesized from the reviewed adjoint, reduced-order and validation methods.

7. EXPERIMENTAL VALIDATION OF OPTIMIZED COLD PLATES

Confidence is key with geometries generated on their own, and it's essential to have experimental evidence. Two TO problems were considered with the use of liquid-cooled heat sinks: a flow distribution problem that minimized power dissipation with flow-rate quality constraints, and a heat exchange maximization problem under a constant input power constraint [16]. Optimized heat sinks and a conventional S-

shaped channel heat sink were produced and both numerical and experimental studies were conducted. The flow-distribution design also produced the lowest hydraulic resistance, while the heat-exchange design maintained a minimum thermal resistance, so that the objective of the design is the one that limits the capacity of the pump on a given platform.

This related multi-objective formulation dealt with the balance of fluid power dissipation with heat exchange and resulted in cooling channels for either a uniform single heat load or non-uniform multiple heat loads, which are similar to multi-chip power modules [17]. The effect of initial guess, Reynolds number and weighting factors on the Pareto-optimal solutions was investigated, and then full scale 3D conjugate heat transfer simulation was performed, yielding lower thermal resistance and higher Nusselt numbers compared to a conventional parallel channel. Both designs were computer numerically controlled (CNC) machined, and the enhanced performance of the optimized channel was verified experimentally. The data in Table 5 show the validation evidence communicated throughout the corpus.

Table 5. Validation Evidence for Autonomously Generated Cooling Structures

Ref.	Configuration	Baseline	Validation route	Reported outcome
[10]	Pseudo-3D forced-convection heat sink	Size-optimized parallel fins	Body-fitted 2D and 3D simulation	Up to 13.6% lower thermal resistance
[16]	Two TO liquid-cooled heat sinks	S-shaped channel	CNC prototypes and experiments	Lowest hydraulic resistance or lowest thermal resistance, by objective
[17]	Multi-objective TO channel	Parallel channel	3D CHT and CNC experiments	Lower thermal resistance and higher Nu
[18]	Pin-fin EV inverter heat sink	Initial design	CFD of design variants	Effects of pin number, size and flow rate evaluated
[19]	TO integrated with microchannels	Straight microchannel; separate TO	Validated 3D numerical model	−4.28 K peak temperature; −319.42 Pa
[20]	Transient pseudo-3D water-cooled design	Reference design	Comparison with full 3D model	66.7% lower pumping power

Note: Nu = Nusselt number.

Application studies show the extent of the gap between industrial practice and the methodological frontier. Estimating continuous-load power losses, and subsequently testing a series of variants using computational fluid dynamics (CFD) [18] of a pin-fin heat-sink design, the design of a liquid-cooled pin-fin heat sink was carried out for a high-voltage electric-vehicle inverter based on silicon-carbide (SiC) MOSFET or IGBT power modules. This parametric process is clear and widely embraced in engineering companies, but it sees only a small part of the design landscape. When compared with the optimisation-based designs in Table 5, there is significant design space that has yet to be tapped into with regards to production inverter cooling.

8. DISCUSSION

8.1 Emerging Hybrid Designs

A new trend is the hybridisation of topology optimised areas with the use of conventional microchannels. The integrated cold plate minimized the maximum chip temperature and the pressure drop between the chip and the fluid, and reduced the average power dissipation, and enhanced the uniformity of the chip temperature in a 2D design space, compared to the straight microchannel; the maximum chip temperature was reduced by 4.28 K and

the pressure drop was reduced by 319.42 Pa in integrated cold plate while compared to the straight microchannel [19]. The benefits of hybridization include maintaining the uniform flow and manufacturability of microchannels while taking advantage of the design flexibility of TO, and they have been found suitable for electric-vehicle power modules and aerospace electronics. The percentage improvements across the corpus is compared in Figure 6.

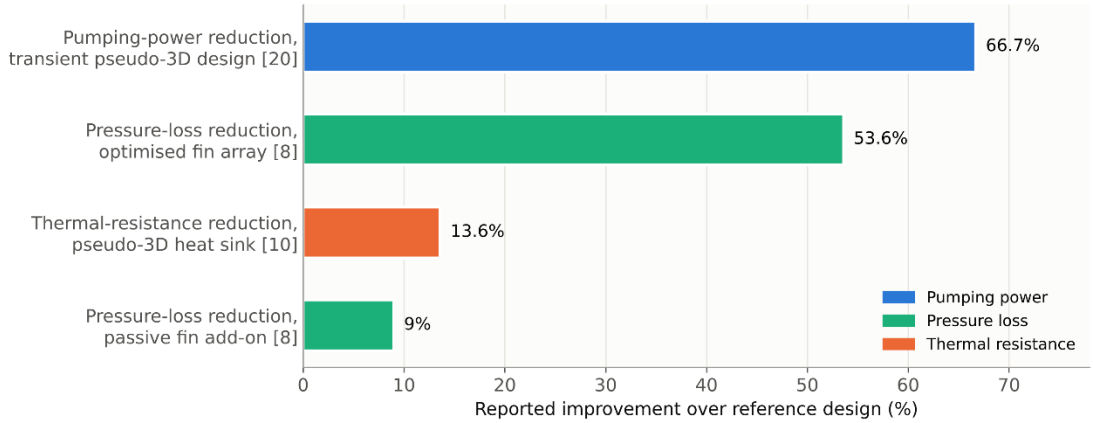


Figure 6. Reported Percentage Improvements of Optimized Cooling Structures Over Reference Designs

Note: absolute results without a percentage basis (4.28 K and 319.42 Pa) are listed in Table 5.

8.2 *Challenges and Outlook*

Transient Optimization is the most direct connection to mobility duty cycles. The heat removal was minimized (to a prescribed period at the end of the operation) by means of a transient pseudo-three dimensional thermofluid model, the layers being coupled by an artificial convection coefficient, with the water-cooled design yielding better instantaneous thermal performance as well as a reduction of 66.7% in pumping power compared to the reference design [20]. Notwithstanding these advances, the corpus shows that there are still significant gaps, such as structural compliance, thermal-cycling fatigue and coolant-pressure loading, which are not continually checked within the optimization process; minimum-feature and manufacturing constraints are applied only post optimization; and validation using realistic drive cycles is not common. These challenges are mapped to the range of mitigation routes supported by the reviewed evidence in Table 6.

Table 6. Challenges, Evidence and Mitigation Routes for Thermo-Mechanical Co-Design

Challenge	Evidence in corpus	Mitigation route	Priority
Structural constraints absent from the loop	Mechanics treated implicitly through volume fraction	SIMP compliance constraint (13)–(14) within the adjoint loop [14]	High
Cost of 3D, transient and turbulent models	15–20 min per 2D iteration and up to 18 GB memory [8]	Pseudo-3D reduced-order models [10], [20]	High
Laminar-dominated literature	Most of 186 surveyed papers treat steady laminar flow [2]	Turbulent density-based TO [7]	Medium
Manufacturability of fine features	CNC-machined prototypes [16], [17]	Hybrid TO and microchannel layouts [19]	High
Selection of the fin family	Plate-fin versus pin-fin regime dependence [13]	Operating-point screening before TO	Medium

Challenge	Evidence in corpus	Mitigation route	Priority
Drive-cycle transients	Steady objectives dominate	Transient objectives such as (5) [6], [15], [20]	High
Industrial adoption	Parametric practice in inverter design [18]	Experimentally validated TO workflows [16], [17]	Medium

Note: priority reflects the synthesized impact on mobility-platform deployment.

9. CONCLUSION

This systematic review collated 20 studies on the autonomous design of embedded liquid-cooled structures and explained their results in terms of high power mobility platforms. Density based TO with Brinkman penalization has progressed to a viable autonomous design engine with the aid of adjoint sensitivities and reduced-order pseudo-three-dimensional models. It delivers consistent benefits: up to a 53.6% reduction in pressure loss for optimized fin arrays, up to a 13.6% reduction in thermal resistance compared to size optimized fins, a 66.7% reduction in pumping power in a transient design and a 4.28K reduction in peak temperature in a hybrid cold plate. Conventional cooling equipment already accounts for 14% to 33% of the traction-inverter size, so these benefits directly correspond to higher power densities.

The main disadvantage of the current state of the art is that thermo-mechanical co-design is still largely aspirational. Optimization rarely takes into account structural compliance, thermal cycling fatigue, coolant pressure loading and manufacturing limitations, and drive cycles are rarely represented as transients. The closed-loop approach is suggested in this review to overcome these shortcomings by combining mission profiles, reduced order multiphysics solvers, adjoint updates, and structural constraints and experimental verification. Further research is needed that focuses on turbulent and transient formulations of the problem containing compliance limits, systematic experimental benchmarks with representative vehicle loading, and hybrid topologies that balance optimal design with manufacturability.

REFERENCES

[1] A. Abdoli, G. Jimenez, and G. S. Dulikravich, "Thermo-fluid analysis of micro pin-fin array cooling configurations for high heat fluxes with a hot spot," *International Journal of Thermal Sciences*, vol. 90, pp. 290–297, 2015, doi: 10.1016/j.ijthermalsci.2014.12.021.

[2] J. Alexandersen and C. S. Andreasen, "A review of topology optimisation for fluid-based problems," *Fluids*, vol. 5, no. 1, Art. no. 29, 2020, doi: 10.3390/fluids5010029.

[3] Y. Alihosseini, M. Z. Targhi, M. M. Heyhat, and N. Ghorbani, "Effect of a micro heat sink geometric design on thermo-hydraulic performance: A review," *Applied Thermal Engineering*, vol. 170, Art. no. 114974, 2020, doi: 10.1016/j.applthermaleng.2020.114974.

[4] H. T. Chen, P. L. Chen, J. T. Horng, and Y. H. Hung, "Design optimization for pin-fin heat sinks," *Journal of Electronic Packaging*, vol. 127, no. 4, pp. 397–406, 2005, doi: 10.1115/1.2056572.

[5] T. Dbouk, "A review about the engineering design of optimal heat transfer systems using topology optimization," *Applied Thermal Engineering*, vol. 112, pp. 841–854, 2017, doi: 10.1016/j.applthermaleng.2016.10.134.

[6] Y. Deng, Z. Liu, P. Zhang, Y. Liu, and Y. Wu, "Topology optimization of unsteady incompressible Navier–Stokes flows," *Journal of Computational Physics*, vol. 230, no. 17, pp. 6688–6708, 2011, doi: 10.1016/j.jcp.2011.05.004.

[7] S. B. Dilgen, C. B. Dilgen, D. R. Fuhrman, O. Sigmund, and B. S. Lazarov, "Density based topology optimization of turbulent flow heat transfer systems," *Structural and Multidisciplinary Optimization*, vol. 57, no. 5, pp. 1905–1918, 2018, doi: 10.1007/s00158-018-1967-6.

[8] A. Ghasemi and A. Elham, "A novel topology optimization approach for flow power loss minimization across fin arrays," *Energies*, vol. 13, no. 8, Art. no. 1987, 2020, doi: 10.3390/en13081987.

[9] A. Ghasemi and A. Elham, "Multi-objective topology optimization of pin-fin heat exchangers using spectral and finite-element methods," *Structural and Multidisciplinary Optimization*, vol. 64, no. 4, pp. 2075–2095, 2021, doi: 10.1007/s00158-021-02964-6.

[10] J. H. Haertel, K. Engelbrecht, B. S. Lazarov, and O. Sigmund, "Topology optimization of a pseudo 3D thermofluid heat sink model," *International Journal of Heat and Mass Transfer*, vol. 121, pp. 1073–1088, 2018, doi: 10.1016/j.ijheatmasstransfer.2018.01.078.

[11] F. Hajabdollahi, H. H. Rafsanjani, Z. Hajabdollahi, and Y. Hamidi, "Multi-objective optimization of pin fin to determine the optimal fin geometry using genetic algorithm," *Applied Mathematical Modelling*, vol. 36, no. 1, pp. 244–254, 2012, doi: 10.1016/j.apm.2011.05.048.

[12] S. Jones-Jackson, R. Rodriguez, Y. Yang, L. Lopera, and A. Emadi, "Overview of current thermal management of automotive power electronics for traction purposes and future directions," *IEEE Transactions on Transportation Electrification*, vol. 8, no. 2, pp. 2412–2428, 2022, doi: 10.1109/tte.2022.3147976.

[13] S. J. Kim, D. K. Kim, and H. H. Oh, "Comparison of fluid flow and thermal characteristics of plate-fin and pin-fin heat sinks subject to a parallel flow," *Heat Transfer Engineering*, vol. 29, no. 2, pp. 169–177, 2008, doi: 10.1080/01457630701686669.

[14] E. Kontoleontos, E. Papoutsis-Kiachagias, A. Zymaris, D. Papadimitriou, and K. Giannakoglou, "Adjoint-based constrained topology optimization for viscous flows, including heat transfer," *Engineering Optimization*, vol. 45, no. 8, pp. 941–961, 2013, doi: 10.1080/0305215X.2012.717074.

[15] S. Kreissl, G. Pingen, and K. Maute, "Topology optimization for unsteady flow," *International Journal for Numerical Methods in Engineering*, vol. 87, no. 13, pp. 1229–1253, 2011, doi: 10.1002/nme.3151.

[16] H. Li, X. Ding, D. Jing, M. Xiong, and F. Meng, "Experimental and numerical investigation of liquid-cooled heat sinks designed by topology optimization," *International Journal of Thermal Sciences*, vol. 146, Art. no. 106065, 2019, doi: 10.1016/j.ijthermalsci.2019.106065.

[17] H. Li, X. Ding, F. Meng, D. Jing, and M. Xiong, "Optimal design and thermal modelling for liquid-cooled heat sink based on multi-objective topology optimization: An experimental and numerical study," *International Journal of Heat and Mass Transfer*, vol. 144, Art. no. 118638, 2019, doi: 10.1016/j.ijheatmasstransfer.2019.118638.

[18] A. Suresh, N. Jinesh, J. K. Antony, and A. Issac, "Design of liquid cooled pin–fin heat sink for high voltage electric vehicle," in *Fluid Mechanics and Fluid Power, Volume 1* (Lecture Notes in Mechanical Engineering), K. M. Singh, S. Dutta, S. Subudhi, and N. K. Singh, Eds. Springer, 2024, doi: 10.1007/978-981-99-7827-4_18.

[19] N. Wang, B. Tian, L. Liu, J. Li, and S. Shao, "Integrated topology optimization and microchannel cold plate for chip cooling," *Energy Proceedings*, vol. 58, 2025, doi: 10.46855/energy-proceedings-11863.

[20] T. Zeng, H. Wang, M. Yang, and J. Alexandersen, "Topology optimization of heat sinks for instantaneous chip cooling using a transient pseudo-3D thermofluid model," *International Journal of Heat and Mass Transfer*, vol. 154, Art. no. 119681, 2020, doi: 10.1016/j.ijheatmasstransfer.2020.119681.